Global survey of lunar wrinkle ridge formation times

Authors: Z. Yue [1], G. Michael [2], K. Di [1,*], J. Liu [3]

Affiliations:

[1] State Key Laboratory of Remote Sensing Science, Institute of Remote Sensing and Digital Earth Chinese Academy of Sciences, Beijing, China 100101.

[2] Institute of Geological Sciences, Freie Unversitaet Berlin, Malteser Strasse 74-100, Haus D, Berlin, Germany 12249

[3] Institute of Geochemistry Chinese Academy of Sciences, Guiyang, China 550002.

*Correspondence to: Kaichang Di. Email: dikc@radi.ac.cn; Tel: 8610-64868229

Address: P. O. Box 9718, Datun Road, Chaoyang District, Beijing, 100101, China

Highlights:

1. We demonstrate a new approach to date lunar wrinkle ridges
2. A global survey of wrinkle ridges ages was made using buffered crater counting
3. Ridge groups show average ages between 3.5 and 3.1 Ga, typically around 0.5 Ga after emplacement of oldest local mare basalts

Abstract:

Wrinkle ridges are a common feature of the lunar maria and record subsequent contraction of mare infill. Constraining the timing of wrinkle ridge formation from crater counts is challenging because they have limited areal extent and it is difficult to determine whether superposed craters post-date ridge formation or have alternatively been uplifted by the deformation. Some wrinkle ridges do allow determination to be made. This is possible where a ridge shows a sufficiently steep boundary or scarp that can be identified as deforming an intersecting crater or the crater obliterates the relief of the ridge. Such boundaries constitute only a small fraction of lunar wrinkle ridge structures yet they are sufficiently numerous to enable us to obtain statistically significant crater counts over systems of structurally related wrinkle ridges. We carried out a global mapping of mare wrinkle ridges, identifying appropriate boundaries for crater identification, and mapping superposed craters. Selected groups of ridges were analyzed using the buffered crater counting method. We found that, except for the ridges in mare Tranquilitatis, the ridge groups formed with average ages between 3.5 and 3.1 Ga ago, or 100–650 Ma after the oldest observable erupted basalts where they are located. We interpret these results to suggest that local stresses from loading by basalt fill are the principal agent responsible for the formation of lunar wrinkle ridges, as others have proposed. We find a markedly longer interval before wrinkle ridge formation in Tranquilitatis which likely indicates a different mechanism of stress accumulation at this site.

Keywords: Lunar Wrinkle Ridges
Age Determination
Buffered Crater Counting

1. Introduction

Lunar wrinkle ridges are linear to sinuous landforms on the lunar surface (Strom, 1972; Bryan, 1973; Maxwell et al., 1975; Chicarro et al., 1985), and most of them occur in maria basins (Plescia and Golombek, 1986; Watters and Johnson, 2010) except a few extending into nearby highlands (Maxwell et al., 1975; Plescia and Golombek, 1986). Lunar wrinkle ridges typically consist of a broad arch and a superposed sharper ridge although the detailed morphologies can vary to a large extent (e.g., Strom, 1972; Sharpton and Head, 1988). This enables them be distinguished from the surrounding terrains by the change in slope (Golombek et al., 1991).

The debate on the lunar ridges being of tectonic or volcanic origin gradually reached the consensus (see the reviews by Sharpton and Head, 1988) that they result from tectonism (e.g., Ono et al., 2009; Watters and Johnson, 2010). However, understanding of the mechanisms that control their development is less well agreed upon, for example, the depth of faulting or whether wrinkle ridges are an expression of thick- or thin-skinned deformation (e.g., Watters, 1991; Mangold et al., 1998; Montési and Zuber, 2003a, 2003b), and the stress field(s) responsible for their formation (Mangold et al., 2000). Another important issue is constraining the time periods over which they were formed. In previous studies, Fagin et al. (1978) argued that ridge formation reflects a late stage in the deformation of the lunar surfaces, and then proposed that ridges in Maria Crisium, Imbrium, Serenitatis, and Tranquilitatis developed beginning from 3.8 – 2.5 Ga. By analyzing the stratification in the Serenitatis basin, Ono et al. (2009) showed that lunar ridges formed after 2.84 Ga. Watters and

Johnson (2010) proposed that lunar wrinkle ridges continued to form as recently as 1.2 Ga ago. All of these works infer the possible ages of the ridges from upper/lower bounds. In an effort to tighten the uncertainty associated with their ages, we attempt to determine ridge ages directly using the buffered crater counting method.

Crater counting has long been used to determine the age of units of the lunar surface (e.g., Shoemaker et al., 1962). The rationale of the approach is to fit the observed crater size-frequency distribution (SFD) of a given surface unit to a known crater production function (PF) (e.g., Hiesinger et al., 2000; Michael and Neukum, 2010), which is further used to derive the absolute ages along with a chronology function (CF) calibrated to radiometric dating from lunar samples (Stöffler and Ryder, 2001). There are various uncertainties in the procedure arising from the methods used to determine the production function and the subsequent calibration of the chronology function from radiometric samples, which requires inferring the source locations for components of returned samples. Further difficulties occur in identifying the crater population resulting from the primary impactor flux; the population may suffer losses through removal processes (e.g. Hartmann, 1971; Melosh, 2011; Michael and Neukum, 2010), such as material diffusion by impact gardening at small scales or viscous relaxation at large scales, or be contaminated by fragmented or secondary impactors (McEwen et al, 2005; McEwen and Bierhaus, 2006; Ivanov, 2006). Nevertheless, crater statistics measurements have yielded a series of predictions later verified by other techniques (Fassett, 2016), and have been broadly applied to date planetary surfaces achieving results consistent with the observed stratigraphy (e.g. Tanaka et al., 2014).

Normally, the procedure involves mapping the surface unit and identifying the craters that are superposed on it. When applying this method to dating lunar ridges, however, many craters within the mapped area of the ridges could have been formed prior to ridges themselves and have been uplifted during ridge formation. Therefore, to date the ridges with craters which unambiguously post-date the features, we developed a method whereby we map selected boundaries of wrinkle ridges where craters can be identified that either postdate these boundaries or are cut by them. A detailed description of the method will be presented below. In principle, this method should provide ages for lunar wrinkle ridges with a level of uncertainty comparable to that of conventional crater dating for a surface area.

2. Data and the Buffered Crater Counting Method

Using a global mosaic of images from the Lunar Reconnaissance Orbiter Camera (LROC) wide-angle camera (WAC), Yue et al. (2015) mapped the population of wrinkle ridges on the Moon. To remove effects from lighting bias, a hillshade map from the Lunar Orbiter Laser Altimeter (LOLA) data was also used in the mapping. The lunar ridges are categorized into many groups based on their locations and spatial continuity. In our work we assumed that each group of lunar wrinkle ridges within a particular area were formed by the same geologic process and thus have a roughly uniform age, and sometimes make sub-divisions where breaks in the structural orientation or spatial

continuity of the ridges are observed.

To date the wrinkle ridges, we need to identify a population of impact craters that was emplaced after the ridges formed and relate it to an appropriate accumulation area: this allows us to find the population density required for the chronology model. Close examination of the ridges reveals that many craters intersect them, but it is often not possible to determine whether a crater formed before or after the ridge itself. A crater uplifted during ridge formation may appear very similar to one which was emplaced on top of the ridge structure. We therefore restricted our analysis to portions of the ridges showing scarps or well-defined steep scarp-like boundaries. In such cases, we were able to identify whether a crater cuts the scarp – indicating that the crater formed later – or the scarp cuts the crater, indicating that the crater was pre-existing. Scarps are associated with mapped wrinkle ridges sufficiently often that we may expect they provide a good local sampling of the superposed crater population.

Image data for the study were drawn from the Lunaserv mapserver LROC NAC overlay (Estes et al., 2013) at 2048 pixels/degree, equivalent to about 15 m/pixel, to cover the area of ridges previously mapped by Yue et al. (2015). The ridges were re-mapped at this resolution, and portions of the ridge boundaries showing scarps or pronounced steep boundaries were marked with polylines in a GIS system. Superposed craters were mapped using CraterTools to determine the crater diameter correctly with regard to the map projection (Kneissl et al, 2011). We used a simplified buffering scheme compared to that described by Kneissl et al. (2015), calculating the buffer area as the product of the polyline length and crater diameter. However, the intent was the

same: to reference each crater to a buffer area around the polylines, representing the area where we would have been able to identify other superposing craters of the same diameter if they were present. Since the scarps show limited local curvature, the simplified approach is a good approximation, and avoids the very large computational effort of calculating geodesic buffers around such a large number of features. The simplified approach is valid so long as the buffer areas of adjacent mapped sections do not intersect, which could occur if scarps are present on both sides of a wrinkle ridge. Where we observed such configurations, we chose to map only one of the boundaries, typically selecting the more prominent or longer side. Given that we are working from the assumption that spatially associated ridges formed together – especially the two sides of a single ridge – we do not expect this selection to bias the measured population.

Each scarp-intersecting crater was examined and included only if judged to post-date the scarp formation. Figure 1 illustrates scarp-intersecting craters in Mare Imbrium and Mare Serenitatis. Figure 1a shows a narrow ridge interrupted by three younger craters as shown in Figure 1b. The polyline was constructed along a steep boundary segment of the ridge as seen from the image: it represents a path where we are confident that we would have been able to identify superposed craters if they were present. To calculate a crater density, we determined the accumulation area, which is the product of the polyline length and the crater diameter (Tanaka, 1982; Fassett and Head, 2008; Kneissl et al., 2015). To obtain good statistics, we compiled the results from all the ridges within a basin, sometimes making sub-divisions where breaks in the structural orientation or spatial continuity of the ridges may indicate that a different stress field

may have acted. Figure 2 shows the groupings we made represented with different colours: generally they are grouped by basin, but in some cases there are further divisions within a basin (different shades of same colour). The exact divisions may be found in the shape files in the supporting data.

Figures 1c and 1d show an example where the craters were formed earlier than the ridge in Mare Serenitatis. The three marked craters were modified by the ridge formation. These craters are excluded from the counts used to date the ridges in this research.

The strategy of only using the craters along scarp-like boundaries of the lunar ridges allows us to avoid the result being contaminated by craters which pre-date the wrinkle ridges. It does, however, limit the number of countable intersecting craters available for the dating statistics. As a result, we can only derive the ages of nine groups of lunar wrinkle ridges with confidence as shown subsequently (Figure 3 and Table 1). In our work, groups of lunar wrinkle ridges were always associated with more craters than in other recent publications (e.g., Xiao and Strom, 2012; Kneissl et al., 2015).

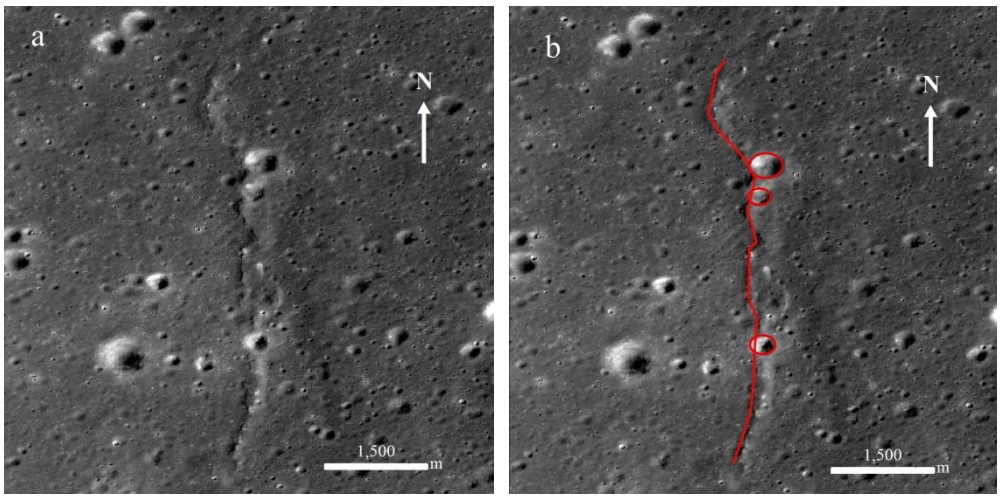

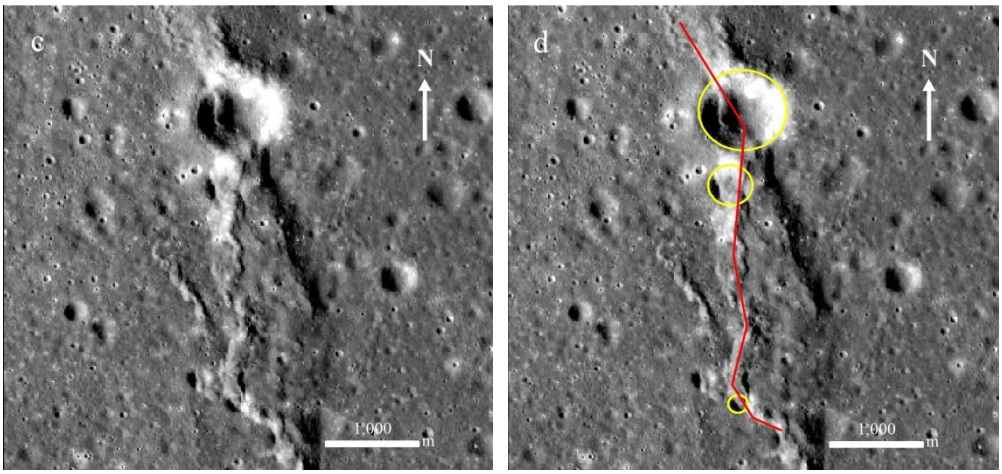

Figure 1. Examples of craters which (a,b) post-date (red circles, 19.1°W 42.6°N, Mare Imbrium) and (c,d) pre-date (yellow circles, 11.1°E 24.9°N, Mare Serenitatis) wrinkle ridge formation. Images from Lunaserv mapserver LROC NAC overlay (Estes et al., 2013).

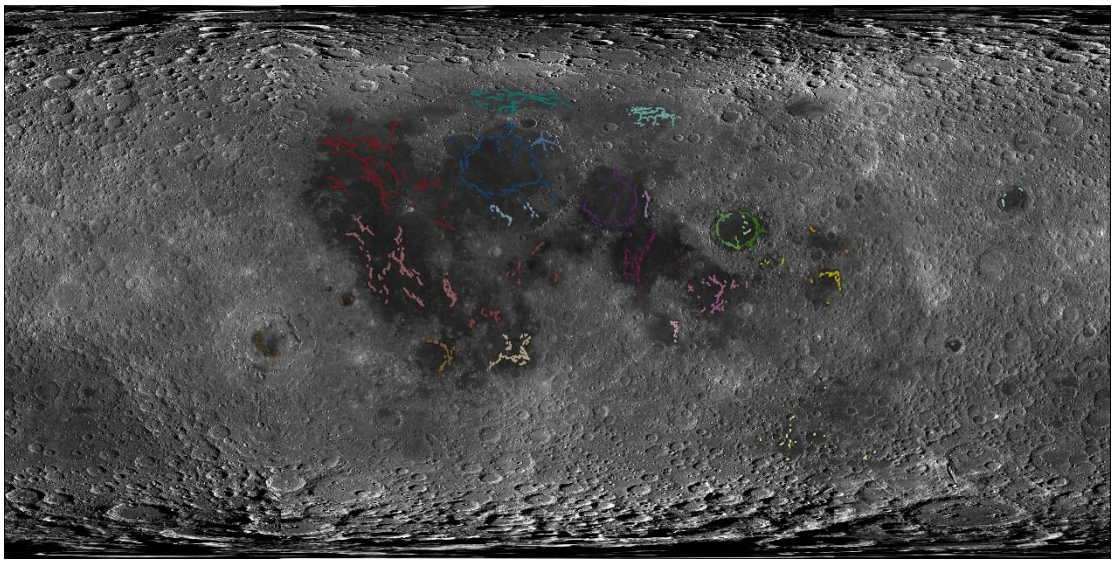

Figure 2. Mapped wrinkle ridge scarps overlaid on LROC WAC mosaic. Note that only portions of the ridges where we interpret the slope to be sufficiently steep to enable identification of the superposition relationship with intersecting craters are shown. Colours represent groups of ridges which were aggregated for analysis.

Absolute ages were determined from the buffered crater counts in the conventional manner, i.e., fitting the differential form of the lunar production function to the range of data points consistent with it, and deriving the age from the measured population density through the chronology function (Neukum, 1983; Michael, 2013).

3. Results

Table 1 lists the results of our mapping and analysis, including the total length of the mapped ridge segments, the number of post-dating craters, and the derived age of each group of ridges. Figure 3 plots the ages found for the nine groups of lunar wrinkle ridges, with the Group ID corresponding to the names in Table 1. The quoted errors relate to the Poisson statistics of the chronology model and do not include the uncertainty of calibration of the chronology model itself.

According to the derived model ages for the nine groups of lunar ridges, the wrinkle ridges in maria Fecunditatis and Crisium are the oldest with the model ages of 3.52 Ga and 3.51 Ga. All of these ridge systems were formed from Late Imbrian to Early Eratosthenian.

The ridge system in Tranquilitatis which, notably, is not concentric to the basin as for the neighbouring mascon basins Serenitatis and Crisium, yielded a formation time of 2.4 Ga, that is 1.4 Ga after its oldest surface lavas.

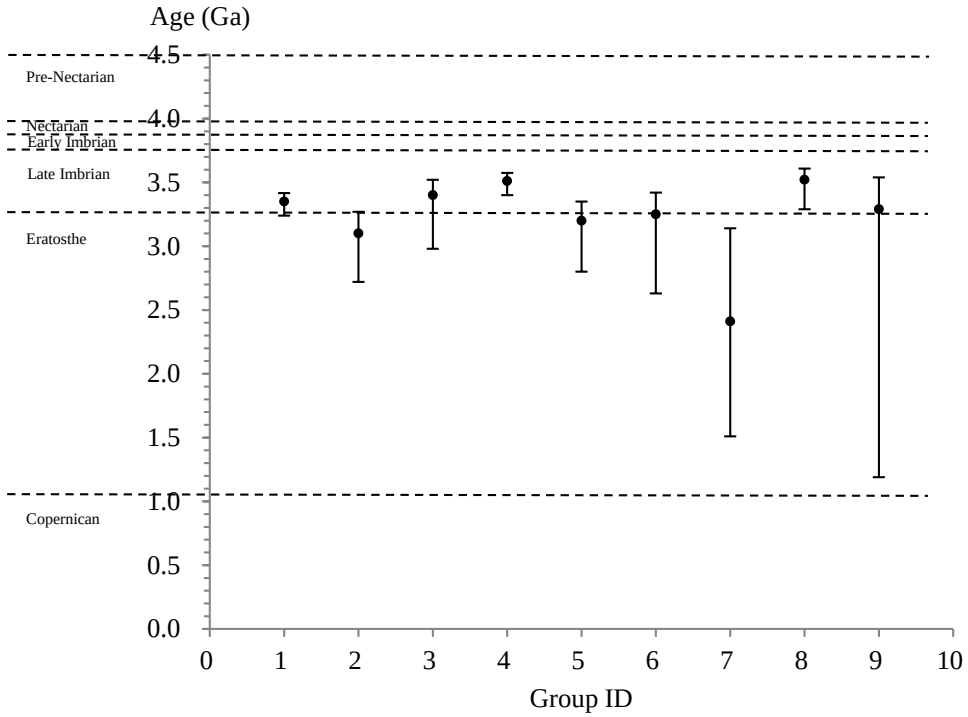

Figure 3. Summary of geologic ages of eight groups of lunar wrinkle ridges, against the Wilhelms (1987) geologic timescale. The groups of lunar wrinkle ridges are denoted from left to right according to the number of craters available for dating (group ID corresponds to names in Table 1). Error bars are 1-sigma and relate to the Poisson statistics of the chronology model, not including the uncertainty of calibration of the chronology model itself.

Table 1. Age measurements for eight groups of lunar wrinkle ridges.

Group ID	Group Name	Center Location	Mapped Ridge Length (km)	Counted crater number	Ages (Ga)

1	Oceanus Procellarum	57.38° W, 18.42° N	9148.9	1358	$3.35^{+0.067}_{-0.11}$
2	Imbrium	16.28° W, 38.36° N	4508.3	629	$3.10^{+0.17}_{-0.38}$
3	Serenitatis	18.08° E, 26.00° N	1717.5	307	$3.40^{+0.12}_{-0.42}$
4	Crisium	58.28° E, 17.64° N	1713.7	275	$3.51^{+0.064}_{-0.11}$
5	Frigoris	14.6° W, 59.3° N	2854.0	244	$3.20^{+0.15}_{-0.40}$
6	Nubium	16.60° W, 21.30° S	1218.1	218	$3.25^{+0.17}_{-0.62}$
7	Tranquilitatis	34.32° E, 6.18° N	890.9	200	$2.41^{+0.73}_{-0.90}$
8	Fecunditatis	50.28° E, 2.50° S	1175.9	89	$3.52^{+0.088}_{-0.23}$
9	Humorum	40.55° W, 23.66° S	568.9	72	$3.29^{+0.25}_{-2.1}$

Figure 4 shows the crater size frequency distributions (CSFDs) of all the groups of ridges in this global survey (the same data is given in R-plot form in online supporting Figure S1). In those basins where we identified structurally or spatially distinct sub-groups of ridges, we found no significant difference in the superposed crater populations. We show the sub-group data in Figure 4 with alternative symbols, but the ages are measured in each case from the aggregate of the whole basin (shown with solid circles). For the maria Australe, Grimaldi, Moscoviense, Nectaris, Orientale, Smythii, Undarum, and Marginis, the data were insufficient to make isochron fits, but we note that the populations nevertheless appear generally consistent with those where we could.

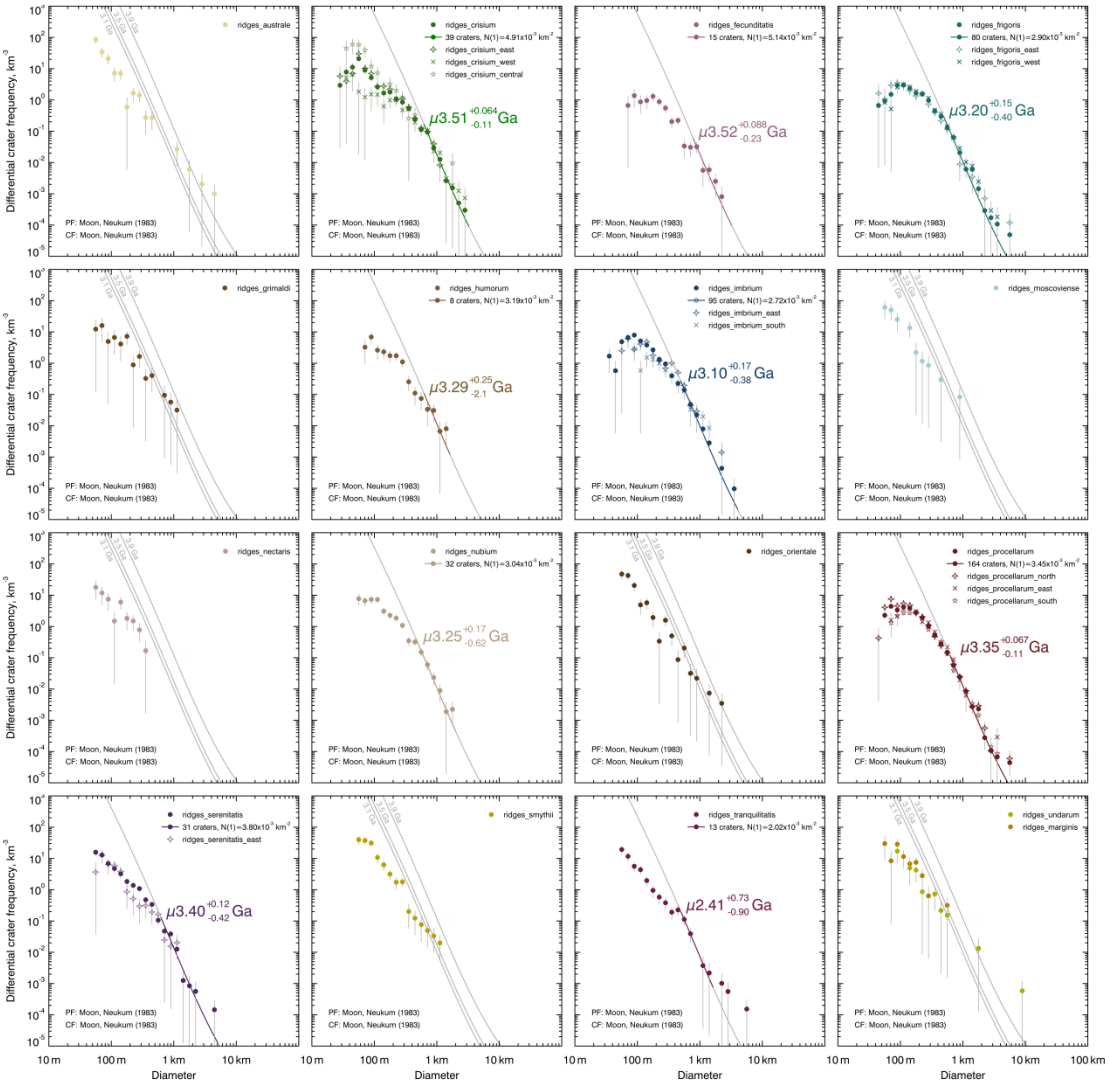

Figure 4. The CSFDs and derived model ages of the lunar wrinkle ridge systems in Table 2. μ is a function representing the uncertainty of calibration of the chronology model (Michael et al., 2016). The groups and sub-divisions are corresponding to the field of group in the supported online shapefiles.

4. Discussions

In our work, we determined the ages of lunar wrinkle ridges directly, where previously they were only loosely constrained by the ages of the surfaces they deform. Fagin et al. (1978) recorded that the ridges in maria Crisium, Imbrium, and Serenitatis

occur on surfaces aged between 3.8 and 2.5 Ga, noting that they may have continued developing up to the present since they are seen to deform small craters in eastern Mare Serenitatis as well as the landslide material crossing the Lee-Lincoln scarp at the Apollo 17 landing site. Ono et al. (2009), by studying the relationship between buried regolith layers and subsequent basalt deposition from radar sounding, proposed that the ridge formation was dominantly produced by global cooling, and occurred after 2.84 Ga. Based on stratigraphic constraints that the youngest mare basalt units have been deformed by the wrinkle ridges, Watters and Johnson (2010) derived that formation of wrinkle ridges continued at least until as recently as ~1.2 Ga ago..

Our results indicate average formation times of 3.5 Ga for Mare Crisium, 3.4 Ga for Serenitatis, and 3.1 Ga for Imbrium, placing the majority of contraction close to the beginning of the previously constrained intervals. To analyze the temporal relation between the lunar maria and the wrinkle ridges, we made a summary of the formation times of the lunar mare basalts and the derived ages of the corresponding ridge systems (Table 2). The ages of the lunar mare basalts include the duration of all the different units where the basalts are located and, as would be expected, all the measured ridge ages were found to be younger than the lunar basalts upon which they occur. Table 2 also includes the age differences between the oldest basalt units and the ridges. Aside from the ridges in Mare Tranquilitatis, all the other dated groups show formation times 0.10~0.65 Ga after the earliest observable erupted material from the same mare. The development of the lunar wrinkle ridges depends heavily on the thickness or volume of the lunar basalt (Yue et al., 2015), which may last as long as the periods described in

Table 2. Solomon and Head (1979) proposed that subsidence usually continued for some time after the emplacement of flooding, due to the fluid behavior of the mantle.

The recent ridge formation noted by Fagin et al. (1978) would serve, in our analysis, to bring down the average age of the ridge groups. The measured ages being so early, however, indicates that ridge formation was not evenly distributed through time. A reasonable interpretation of our data could be that the majority of ridge formation occurred soon after basalt emplacement, followed by sporadic development at a rather low level. Local stresses from loading by basalt fill are probably the principal agent responsible for the formation of lunar wrinkle ridges as argued by numerous previous studies (e.g., Maxwell, 1975; Melosh, 1978; Freed et al., 2001).

The ridge system in Tranquilitatis which, notably, is not concentric to the basin as for the neighbouring mascon basins Serenitatis and Crisium, yields an average formation time of 2.4 Ga, that is 1.4 Ga after its oldest surface lavas, a significantly longer period than for any other basin. The curvature of the ridges at Tranquilitatis could indicate a more distant centre of deformation, although the more linear trends of wrinkle ridges in Procellarum and Frigoris suggests a different character of stress field is typical in the absence of a mascon. The age discrepancy, however, appears to point to a different stress mechanism acting in this basin.

Table 2. Summary of the formation times of the lunar mare basalts and the corresponding ages of the wrinkle ridges.

The basalt ages include the duration of different units where the ridges are distributed.

Group	Ridge Ages (Ga)	Basalt Ages (Ga)	Difference (Ga)	Reference
Oceanus Procellarum	$3.35^{+0.067}_{-0.11}$	1.20~3.72	0.37	Hiesinger et al. (2003)
Imbrium	$3.10^{+0.17}_{-0.38}$	2.01~3.57	0.47	Hiesinger et al. (2000)
Serenitatis	$3.40^{+0.12}_{-0.42}$	2.44~3.81	0.41	Hiesinger et al. (2000)
Crisium	$3.51^{+0.064}_{-0.11}$	2.71~3.61	0.10	Hiesinger et al. (2011)
Frigoris	$3.20^{+0.15}_{-0.40}$	2.61~3.71	0.51	Hiesinger et al. (2010)
Nubium	$3.25^{+0.17}_{-0.62}$	3.25~3.85	0.60	Hiesinger et al. (2003)
Tranquilitatis	$2.41^{+0.73}_{-0.90}$	3.39~3.80	1.39	Hiesinger et al. (2000)
Fecunditatis	$3.52^{+0.088}_{-0.23}$	3.14~3.68	0.16	Hiesinger et al. (2006)
Humorum	$3.29^{+0.25}_{-2.1}$	2.93~3.94	0.65	Hiesinger et al. (2000)

5. Conclusions

In this research, we demonstrate a new approach to dating lunar wrinkle ridges, based on the crater size-frequency distribution along particular segments of their boundaries where we can unambiguously determine cross-cutting relationships. We use these segments to sample various population groups of ridges, making a systematic survey over all the lunar maria, and applying the buffered crater counting method to estimate the average ages of the groups.

We provided direct measurements of the ages of nine groups of lunar wrinkle

ridges, making use of superposed craters in the size range of 1 km to several kilometers for all groups of lunar wrinkle ridges, such as to minimize the possible effect of contamination by secondary craters, considering the current debate on uncertainties associated with using small craters in dating the lunar surface (Xiao and Strom, 2012).

Our investigation indicates that, except for the ridges in mare Tranquilitatis, typical lunar wrinkle ridge groups have average ages from late Imbrian to early Eratosthenian, or from 3.5 to 3.1 Ga, which is 0.1 – 0.7 Ga later than the eruption of the oldest basalts where they are located. We note that the average ages may be reduced by sporadic development of more recent ridges. Lobate scarps, which in some cases are seen to transition into wrinkle ridges, are known elsewhere to be young features (Watters et al., 2010; Clark et al., 2017). It thus seems not likely that some wrinkle ridge development may also be young.

Our findings are consistent with local stresses from the loading by basalt fill being the main cause of the formation of lunar wrinkle ridges, as others have proposed. We note that the average age of the wrinkle ridges in Mare Tranquilitatis differs from the trend seen elsewhere, which may point to a different stress mechanism having acted in this region.

Acknowledgements

The authors thank Prof. Karl Mueller at University of Colorado for his thoughtful comments which greatly helped us to improve the manuscript. We also gratefully

acknowledge Arizona State University for providing LROC images and mosaic and NASA Goddard Space Flight Center for providing LOLA data products. The authors are grateful to Thomas Kneissl both for his constructive suggestions and the software CraterTools. This work was supported by the National Natural Science Foundation of China (Grant No. 41490635 and 41590851) and by DLR (grant 50QM1301) and the German Research Foundation (DFG) (grant SFB TRR-170-1 A4).

Reference

Bryan, W. B., 1973. Wrinkle ridges as deformed surface crust on ponded mare lava. Proc. Lunar Planet. Sci. Conf., 4, 93–106.

Chicarro, A. F., Schultz, P. H., Masson, P., 1985. Global and regional ridge patterns on Mars. Icarus, 63(1), 153–174, doi:10.1016/0019-1035(85)90025-9.

Clark, J.D., Bogert, C.H. van der, Hiesinger, H., 2015. How Young are Lunar Lobate Scarps? Lunar Planetary Science Conference. p. 1730.

Estes, N. M.; Hanger, C. D., Licht, A.A., Bowman-Cisneros, E., 2013. Lunaserv Web Map Service: History, Implementation Details, Development, and Uses. Lunar Planet. Sci. Conf., 44, abstract 2069.

Fassett, C. I., and Head, J. W., 2008. The timing of martian valley network activity: Constraints from buffered crater counting. Icarus, 195(1), 61–89, doi:10.1016/j.icarus.2007.12.009.

Fassett, C. I., 2016. Analysis of impact crater populations and the geochronology of planetary surfaces in the inner solar system, J. Geophys. Res. Planets, 121, 1900–1926, doi:10.1002/2016JE005094.

Freed, A. M., Melosh, H. J., Solomon, S. C., 2001. Tectonics of mascon loading: Resolution of the strike-slip faulting paradox. J. Geophys. Res., 106(E9), 20,603–20,620, doi:10.1029/2000JE001347.

Golombek, M. P., Plescia, J. B., Franklin, B. J., 1991. Faulting and folding in the

formation of wrinkle ridges. Proc. Lunar Planet. Sci. Conf. 21, 679–693.

Hartmann, W. K., 1971. Martian cratering III: theory of crater obliteration. Icarus, 15, 410–428. doi:10.1016/0019-1035(71)90119-9.

Hiesinger, H., Jaumann, R., Neukum, G., Head III, J. W., 2000. Ages of mare basalts on the lunar nearside, J. Geophys. Res., 105 (E12), 29,239–29,275, doi:10.1029/2000JE001244.

Hiesinger, H., Head III, J. W., Wolf, U., Jaumann, R., , Neukum, G., 2003. Ages and stratigraphy of mare basalts in Oceanus Procellarum, Mare Nubium, Mare Cognitum, and Mare Insularum, J. Geophys. Res., 108(E7), 5065, doi:10.1029/2002JE001985.

Hiesinger, H., Head III, J. W.. Wolf, U.. Jaumann, R.. Neukum. G.. 2006. New ages for basalts in mare Fecunditatis based on crater size-frequency measurements. Lunar Planet. Sci. Conf., 37, abstract 1151.

Hiesinger, H., Head III, J. W., Wolf, U., Jaumann, R., Neukum, G., 2010. Ages and stratigraphy of lunar mare basalts in Mare Frigoris and other nearside maria based on crater size-frequency distribution measurements, J. Geophys. Res., 115, E03003, doi:10.1029/2009JE003380.

Hiesinger, H., van der Bogert, C. H., Reiss, D., Robinson, M. S., 2011. Crater size-frequency distribution measurements of mare Crisium. Lunar Planet. Sci. Conf., 42, abstract 2179.

Ivanov, B. A., 2006. Earth/Moon impact rate comparison: Searching constraints for lunar secondary/primary cratering proportion, Icarus, 183, 504–507, doi:10.1016/j.icarus.2006.04.004.

Kneissl, T., van Gasselt, S., Neukum, G., 2011. Map–projection–independent crater size-frequency determination in GIS environments–New software tool for ArcGIS. Planet. Space Sci., 59(11–12), 1243–1254, doi:10.1016/j.pss.2010.03.015.

Kneissl, T., Michael, G. G., Platz, T., Walter, S. H. G., 2015. Age determination of linear surface features using the Buffered Crater Counting approach - Case studies of the Sirenum and Fortuna Fossae graben systems on Mars. Icarus, 250, 384–394.

Mangold, N., Allemand, P., Thomas, P. G., 1998. Wrinkle ridges of Mars: structural analysis and evidence for shallow deformation controlled by ice-rich décollements. Planet. Space Sci., 46(4), 345–356, doi:10.1016/S0032-0633(97)00195-5.

Mangold, N., Allemand, P., Thomas, P. G., Vidal, G., 2000. Chronology of compressional deformation on Mars: Evidence for a single and global origin. Planet. Space Sci., 48(12–14), 1201–1211, doi:10.1016/S0032-0633(00)00104-5.

Maxwell, T. A., El-Baz, F., Ward, S. W., 1975. Distribution, morphology, and origin of ridges and arches in Mare Serenitatis. Geol. Soc. Am. Bull., 86(9), 1273–1278, doi:10.1130/0016-7606(1975)862.0.CO;2.

McEwen, A. S., and E. B. Bierhaus, 2006. The importance of secondary cratering to age constraints on planetary surfaces, Annu. Rev. Earth Planet. Sci., 34, 535–567, doi:10.1146/annurev.earth.34.031405.125018.

McEwen, A. S., B. S. Preblich, E. P. Turtle, N. A. Artemieva, M. P. Golombek, M. Hurst, R. L. Kirk, D. M. Burr, and P. R. Christensen, 2005. The rayed crater Zunil and interpretations of small impact craters on Mars, Icarus, 176, 351–381, doi:10.1016/j.icarus.2005.02.009.

Melosh, H. J., 1977. Global tectonics of a despun planet. Icarus, 31(2), 221–243. doi:10.1016/0019-1035(77)90035-5.

Melosh, H. J., 1978. The tectonics of mascon loading. Proc. Lunar Planet. Sci. Conf., 9, 3513–3525.

Melosh, H. J., 1980. Tectonic patterns on a tidally distorted planet. Icarus, 43(3), 334–337, doi:10.1016/0019-1035(80)90178-5.

Melosh, H. J., 2011. Planetary surface processes. Cambridge University Press, 534.

Michael, G. G., and Neukum, G., 2010. Planetary surface dating from crater size - frequency distribution measurements: Partial resurfacing events and statistical age uncertainty. Earth Planet. Sci. Lett., 294(3–4), 223–229, doi:10.1016/j.epsl.2009.12.041.

Michael, G. G., 2013. Planetary surface dating from crater size-frequency distribution measurements: Multiple resurfacing episodes and differential isochron fitting. Icarus, 226, 885–890, doi: 10.1016/j.icarus.2016.05.019.

Michael, G. G., Kneissl, T., Neesemann, A., 2016. Planetary surface dating from crater size-frequency distribution measurements: Poisson timing analysis. Icarus, 277,

279–285, doi: 10.1016/j.icarus.2016.05.019.

Montési, L. G. J., and Zuber, M. T., 2003a. Clues to the lithospheric structure of Mars from wrinkle ridge sets and localization instability. J. Geophys. Res., 108(E6), 5048, doi:10.1029/2002JE001974.

Montési, L. G. J., and Zuber, M. T., 2003b. Spacing of faults at the scale of the lithosphere and localization instability: 1. Theory. J. Geophys. Res., 108(B2), 2110, doi:10.1029/2002JB001924.

Neukum, G., 1983. Meteoriten bombardement und Datierung planetarer Oberflachen Habilitation Thesis for Faculty Membership, Univ. of Munich, 186pp. (English translation, 1984: Meteorite bombardment and dating of planetary surfaces. http://ntrs.nasa.gov/search.jsp?R=19840027189).

Ono, T., Kumamoto, A., Nakagawa, H., Yamaguchi, Y., Oshigami, S., Yamaji, A., Kobayashi, T., Kasahara, Y., Oya, H., 2009. Lunar radar sounder observations of subsurface layers under the nearside maria of Moon. Science, 323(5916), 909–912, doi:10.1126/science.1165988.

Plescia, J. B., and Golombek, M. P., 1986. Origin of planetary wrinkle ridges based on the study of terrestrial analogs. Geol. Soc. Am. Bull., 97(11), 1289–1299, doi:10.1130/0016-7606(1986)97<1289:OOPWRB>2.0.CO;2.

Sharpton, V. L., and Head, J. W., 1988. Lunar mare ridges: analysis of ridge-crater intersections and implications for the tectonic origin of mare ridges. Proc. Lunar Planet. Sci. Conf., 18, 307–317.

Shoemaker, E. M., Hackman, R. J., Eggleton, R. E., 1962. Interplanetary correlation of geologic time. Adv. Astronaut. Sci., 8, 70–79.

Solomon, S. C., and Head, J. W. 1979. Vertical movement in mare basins: Relation to mare emplacement, basin tectonics, and lunar thermal history, J. Geophys. Res., 84(B4), 1667–1682, doi:10.1029/JB084iB04p01667.

Stöffler, D., and Ryder, G., 2001. Stratigraphy and isotope ages of lunar geologic units: Chronological standard for the inner solar system. Space Sci. Rev., 96(1–4), 9–54, doi:10.1023/A:1011937020193.

Strom, R. G., 1972. Lunar mare ridges, rings and volcanic ring complexes. Mod. Geol., 2(2), 133–157, doi:10.1007/978-94-010-2861-5_19.

Tanaka, K. L., 1982. A new time-saving crater-count technique, with application to narrow features. NASA Technical Memo, NASA TM-85127, 123–125.

Tanaka, K.L., Skinner Jr., J.A., Dohm, J.M., Irwin III, R.P., Kolb, E.J., Fortezzo, C.M., Platz, T., Michael, G.G., Hare, T.M., 2014. Geologic Map of Mars. U.S. Geological Survey Scientific Investigations Map SIM, 1:20,000,000

Watters, T. R., 1991. Origin of periodically spaced wrinkle ridges on the Tharsis Plateau of Mars. J. Geophys. Res., 96(E1), 15599–15616, doi:10.1029/91JE01402.

Watters, T. R., and Johnson, C. L., 2010. Lunar tectonics. Planetary tectonics, edited by Watters, T. R., Schultz, R. A., 121–182.

Watters, T.R., Robinson, M.S., Beyer, R.A., Banks, M.E., Bell, J.F., Pritchard, M.E., Hiesinger, H., Bogert, C.H. van der, Thomas, P.C., Turtle, E.P., Williams, N.R., 2010.

Evidence of Recent Thrust Faulting on the Moon Revealed by the Lunar Reconnaissance Orbiter Camera. Science 329, 936–940.

Wilhelms, D. E., The geologic history of the Moon,. U.S. Geol. Surv. Prof. Pap., 1348, 302 pp., 1987.

Xiao, Z., and Strom, R. S., 2012. Problems determining relative and absolute ages using the small crater population. Icarus, 220(1), 254–267, doi:10.1016/j.icarus.2012.05.012.

Yue, Z., Li, W., Di, K., Liu, Z., Liu, J., 2015. Global mapping and analysis of lunar wrinkle ridges. J. Geophys. Res. (Planets), 120(5), 978–994, doi:10.1002/2014JE004777.

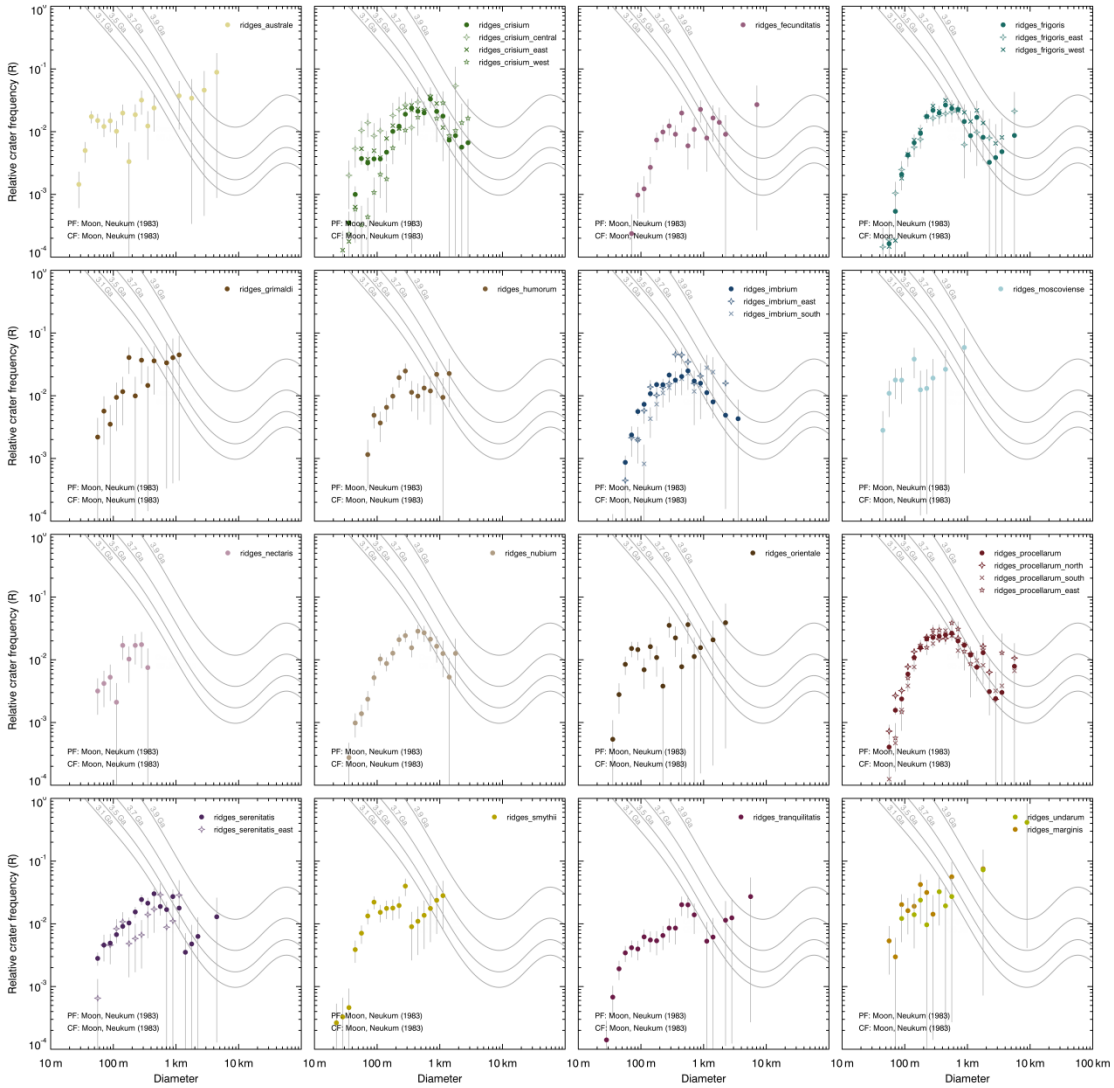

Figure S1. R plot of the crater size–frequency distribution for all groups of lunar ridges. The groups and sub-divisions are responding to the field of *group* in the supported online shapefiles.